

Physical model of C/C coating for anti-ablation protection

Valery V. Alisin *

Mechanical Engineering Research Institute, Moscow, 101990, Russia

Abstract. The article considers the issues of the numerical analysis of the temperature distribution in a powder coating based on zirconium dioxide during the laser melting process. The assumption is substantiated that adding 20% nickel-chrome alloy powder to the coating makes it possible to form a frame structure of the coating, which will increase the strength of the resulting heat-protective coating. Calculation graphs characterizing the temperature and time of propagation of the metal powder melt front along the thickness of the coating are considered. Attention is paid to achieving the melt boundary of the chromium sublayer, which will provide increased adhesive strength of the applied coating. Based on the study, the prospects of the proposed technology for applying a coating to protect against oxidation of carbon composites from the effects of high-speed gas flows, especially for coating large surfaces, are noted.

1 Introduction

Carbon composite materials have a unique combination of specific strength and heat resistance characteristics, and therefore are promising for use in aviation and space technology. The high strength of carbon composite materials makes it possible to manufacture from them power structures of structural supports of devices operating in plasma flows when braking a spacecraft in the atmosphere. However, oxidation and ablation of the material takes place and on the surface flowing over the gas repeatedly or for a long time, so they must be protected. Much attention is paid to the study of the resistance of powder coatings to temperature and mechanical stress. Plasma spraying technology is widely used to apply a protective coating to carbon-carbon composites. Zirconium-based composite powder materials are used in coatings to protect carbon-carbon composites. It has been shown [1, 2] that the coating of the ZrB₂-SiC-Y₂O₃ system is highly resistant to oxidation. Ablation of SiC/SiC composites at ultra-high temperatures using an oxy-acetylene torch flame was studied in [3, 4]. It was found that the removal process was dominated by sublimation and mechanical exfoliation. The work [5] shows that coating technologies are effective methods for solving the problems of oxidation and ablation of carbon composites. The structure of the interface between the coating and the substrate, as well as the anti-oxidation properties of a 774 μm thick coating applied by batch cementation to a carbon composite were studied. The thickness of the sublayer of a multilayer coating determines their service life in critical

* Corresponding author: vva-imash@yandex.ru

conditions. In [6], a multilayer SiC coating with a sublayer on carbon composites using plasma spraying was studied. Multi-stage coating processes are used to improve the resistance of carbon composites to oxidation and thermal shock [7]. The increased thickness coating was obtained by heat treatment at 600°C. Al₂O₃ coatings were obtained by two-stage anodic oxidation. The proposed technology makes it possible to obtain carbon composites with good mechanical properties for operation at high temperatures. In [8], a multicomponent high-entropy boron carbide coating 300 nm thick. In [9, 10], a composite coating based on ZrC was studied. Under conditions of ZrC ablation, a loose ZrO₂ layer with a porous structure is formed. To reduce damage from plasma flames, it has been proposed to add MoSi₂ powder, which increases the resistance of ZrC-based coatings to ablation. To protect carbon fiber materials from ablation, a sublayer of TC₄ coating is used [11]. It is noted that the connection between the TC₄ alloy and carbon composites is critical for aerospace applications. In [12], a ZrO₂ coating stabilized with 6 mol.% Sm₂O₃ was proposed to protect carbon composites from severe oxidation. The mass ablation rate was found to decrease by ~71%. Although there is a lot of research in the field of protecting carbon composites, the problem has not been solved.

The goal is to protect the surface of the carbon composite from oxidation under high temperature.

The task is to investigate the possibility of using zirconium dioxide-based powder coating in the framework of a plastic nickel-chromium matrix to provide thermal protection for a carbon composite.

2 Materials and equipment

The coating of the NiCrBSi with ZrO₂ is applied by a gas-thermal method onto a chromium-metalized carbon composite and melted with a laser. Laser processing technology is performed by a rectangular-shaped light spot formed by 2-axis high-frequency beam scanning with different scanning frequencies. It has been experimentally established that the uneven distribution of energy over the light spot due to the formation of Lissajous figures does not exceed 12%.

3 Results

Let us consider a two-layer semi-bounded body with a coating of thickness h (Figure 1) located on a chromium sublayer, which is exposed to a thermal source with laser radiation power density q_0 , and action time t_H . The energy of laser radiation absorbed by the surface of the body is equal to

$$q_0 = \sum_1^i q_i = q_l - q_{omp} - q_{pl} - q_{ilz} - q_{okis}. \quad (1)$$

where, according to the power density: q_l - laser radiation; q_{orp} - reflected radiation; q_{pl} - absorbed by plasma; q_{ilz} - radiation from the body surface; q_{okis} - released during surface oxidation.

Let us determine the heat fluxes included in equation (1) using the grey box model, which is well applicable to plasma coatings with an oxidized surface:

$$q_{pl} = -\lambda \left(\frac{\partial T}{\partial x} \right)_{x=0} = \alpha (T_S - T_0). \quad (2)$$

$$q_{ilz} = \varepsilon \sigma_0 T_S^4. \quad (3)$$

$$q_{okis} = \frac{Q_{okis}}{S}. \quad (4)$$

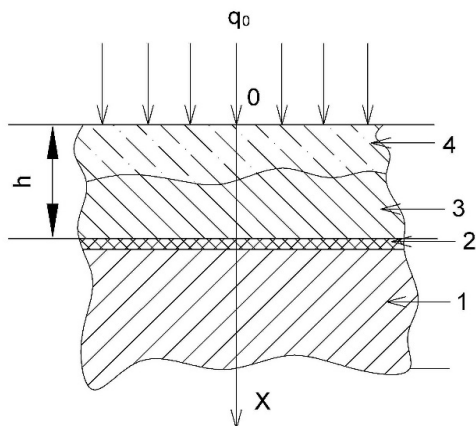


Fig. 1. Scheme for calculating a two-layer semi-bounded body: 1 – carbon composite base, 2 – chromium sublayer, 3 – non-melted part of the coating, 4 – molten coating.

The equation for laminar flow in the boundary layer has the form [13]

$$Nu = \frac{\alpha x}{\lambda} = 0,323 Re^{0,5} Pr^{0,33} \tag{5}$$

where: λ - gas thermal conductivity coefficient; α - heat transfer coefficient;

T_S - body surface temperature in the heating zone (spot); S - heating area;

T_0 - gas temperature outside the boundary layer; ε - degree of body blackness;

σ_0 - Stefan-Boltzmann constant; $Q_{окис}$ - the amount of heat released or absorbed by the surface of a body as a result of oxidation or thermal decomposition; x - current coordinate.

where: Nu , Pr , Re - Nusselt, Prandtl, Reynolds numbers; x – coordinate of the point in question.

It has been experimentally established that the speed of gas movement near the surface of a body $V \leq 15\text{m/s}$, therefore the Reynolds number is:

$$Re = \frac{\rho V x}{\mu} \leq 1,5 * 10^2$$

where: ρ ; μ - density and coefficient of dynamic viscosity of gas.

We have Prandtl number as $Pr = 1$, then the heat transfer coefficient $\alpha = 2,77 * 10^2 \text{ W/(m}^2\text{K)}$.

We determine the fraction of the amount of heat absorbed by the body from the laser radiation power (Q_0)

$$\frac{Q_0}{N_{izl}} = \varepsilon - \frac{\alpha(T_S - T_0)S + \varepsilon\sigma_0 T_S^4 S + Q_{окис}}{N_{izl}} \tag{6}$$

The significance of the terms of equation (1) was assessed with the following values of the variables:

$$\varepsilon = 1; \sigma_0 = 5,67 * 10^{-8} \text{ W/(m}^2\text{K}^4); T_S = 3000^0\text{K}; T_0 = 0; N_{изл.} = 3 * 10^3 \text{ W}; S = 10^{-4} \text{ m}^2. \tag{7}$$

It has been established that while $T_S \leq 2300^0\text{K}$ convective heat transfer and radiation heat flow can be neglected. The response of the material to the action of this source can be found by solving the nonstationary Fourier equation with Stefan boundary conditions.

The heat flow in the spot is described by the normal Gaussian distribution law:

$$q = q_0 \exp(-kr^2). \tag{8}$$

where: k - heat flow concentration coefficient; r - current coordinate.

We obtain the relationship between heat flow (8) and effective radiation power by integrating the heat flow over the surface area:

$$Q = \int_S q_0 \exp(-kr^2) dS = \int_0^\infty q_0 \exp(-kr^2) 2\pi r dr = -\frac{1}{k} q_0 \pi e^{-kr^2} \Big|_0^\infty = \frac{\pi}{k} q_0. \tag{9}$$

Let us introduce into consideration an equivalent heat source with the same power Q , as given (9), but distributed uniformly over a spot of radius r_0 , equal to the largest heat flow q_0 .

$$Q = \pi r_0^2 q_0 = \frac{\pi}{k} q_0; \text{ from which } r_0 = \frac{1}{\sqrt{k}}.$$

Laser power, for equivalent thermal source $q_0 = 2 * 10^7 \dots 3 * 10^7 \text{ W/m}^2$, with diameter $d = 2r_0 = 1,6 * 10^{-2} \text{ m}$, will be $N = (4 \dots 6) / \epsilon k \text{ W}$. These values correspond to the average power of commercially produced laser technological complexes. The concentration coefficient of the specific heat flow of technological lasers is different. k is determined experimentally for each specific laser complex.

Let's determine the thickness of the coating: $h \leq \sum_1^3 h_i = 0,6 * 10^{-3} \text{ m}$.

Where: $h_1 \leq 0,25 * 10^{-3} \text{ m}$ - allowance for dimensional processing, $h_2 \leq 0,25 * 10^{-3} \text{ m}$ - working coating thickness; $h_3 \leq 0,1 * 10^{-3} \text{ m}$ - thickness of the transition zone.

Let's estimate the depth of thermal impact on the base material.

Let us consider the process of heat propagation in a semi-limited body (Figure 1), at a constant temperature on the surface, assuming $a_i = \lambda_i / (\rho_i c_i) = \text{const}$.

Where: λ ; c ; ρ - thermal conductivity, heat capacity, body density, respectively.

The Fourier equation of non-stationary thermal conductivity has the form:

$$\frac{\partial T(x,t)}{\partial t} = a \frac{\partial^2 T(x,t)}{\partial x^2}. \tag{10}$$

Boundary conditions:

- initial condition: $T(x, 0) = 0$.
- boundary condition of the first kind: $T(0, t) = T_S = \text{const}$.

The analytical solution to equation (10), obtained by the method of separation of variables, has the form:

$$\frac{T(x,t)}{T_S} = 1 - \text{erf} \left(\frac{x}{\sqrt{4at}} \right); \tag{11}$$

Gaussian error function

$$\text{erf} z = \frac{2}{\sqrt{\pi}} \int_0^z e^{-\beta^2} d\beta \tag{12}$$

The numerical values of the solution to equation (12) are given in the form of tables in the reference literature.

Let us determine the initial temperature on the surface of the body. Differentiating equation (11) with respect to x , at $t = \text{const}$, we find the value of the temperature gradient at point: $x = 0$:

$$T_S = \frac{q_0 \sqrt{\pi}}{\lambda} (at)^{\frac{1}{2}}.$$

The main assumptions made in the calculation process:

1. A heat source uniformly distributed along the radius r_0 acts on the surface of a two-layer semi-bounded body, $q_0(0, t) = \text{const}$.
2. We consider $a_i = \lambda_i / (\rho_i c_i) = \text{const}$ (the thermal diffusivity coefficient of composite wear-resistant materials and high-strength alloy steel is a constant value).
3. We neglect the specific heat of thermal oxidation and decomposition of the coating material or limit ourselves to the calculation until the $T(x, t) < T_{okis}$ condition is met, (T_{okis} - temperature of intense oxidation or decomposition).
4. We calculate temperature fields until condition $T(x, t) < T_{kip}$ is met, (T_{kip} - boiling point of the coating material).
5. The melting temperature of the coating must satisfy the $T \leq 0,8 \dots 1,0 T_{pl}$ condition, (T_{pl} - melting point of base material).
6. We do not consider hydrodynamic effects in a liquid melt bath.

With the method [13] thermal protection of the surface becomes the main function, and the matrix acts as a frame for retaining ZrO_2 particles. The temperature of the coating surface increases with increasing content of zirconium dioxide particles (Figure 2).

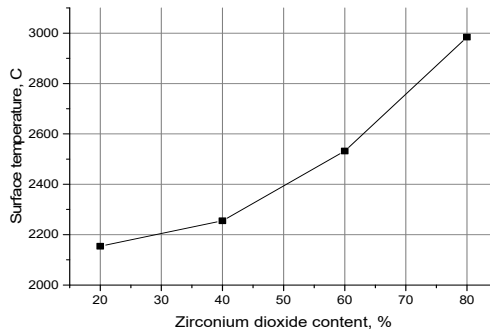


Fig. 2. Effect of zirconium dioxide content on surface temperature.

The coating melting time is reduced in comparison with a lower zirconium dioxide content. When the melting front approaches the nickel substrate, the heating time increases nonlinearly (Figure 3).

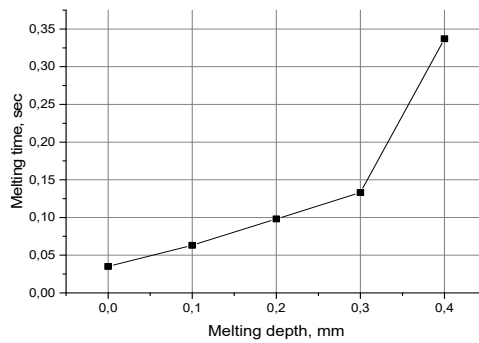


Fig. 3. Effect of melting depth on process time.

Figure 4 shows the temperature distribution over the thickness of the coating when fusing it to a nickel substrate.

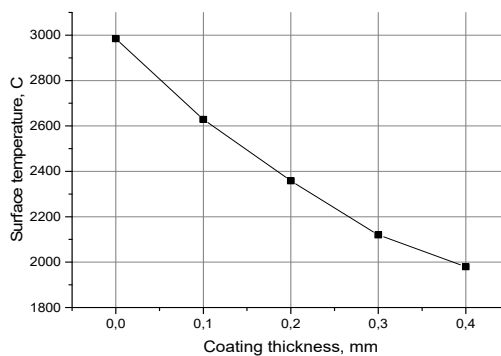


Fig. 4. Effect of melting depth on temperature.

After the melt hardens, a frame of nickel-chromium matrix is formed.

4 Conclusion

The characteristics of thermal fields during laser melting of the heat-protective powder coating ZrO₂ have been established. This makes it possible to determine the technological parameters of laser surface treatment.

The advantage of powder coatings over tile technology is higher performance when protecting large carbon composite surfaces.

The cost of applying powder coating is less than applying heat-protective tiles.

References

1. B. Zhang, M. Yi, Y. Ning, A. Xie, Z. Zhou, Z. Feng, *Corrosion Science* **200**, 110223 (2022).
2. X. Zhang, Y. Zhang, K. Fan, R. Riedel, H. Li, J. Sun, H. Li, *Corrosion Science* **231**, 111944 (2024).
3. J. Du, G. Yu, Y. Jia, Z. Ni, X. Gao, Y. Song, F. Wang, *Corrosion Science* **201**, 110263 (2022).
4. L. Yang, W. Sun, J. Xu, X. Xiong, L. Wang, J. Zuo, B. Yang, *Ceramics International* **50(11)**, Part B 20447-20459 (2024).
5. D. Yang, S. Dong, C. Hong, X. Zhang, *Ceramics International* **48(11)**, 14935-14958 (2022).
6. G. Feng, H. Li, X. Yao, J. Sun, Y. Jia, *J. European Ceramic Society* **42(9)**, 3802-3811 (2022).
7. X. Zhao, P. Wang, J. Zheng, J. Liu, Z. Yang, L. Yang, *Ceramics International* **48(18)**, 26028-26041 (2022).
8. H. Zhang, F. Akhtar, *Surface and Coatings Technology* **425**, 127697 (2022).
9. X. Zhang, Y. Zhang, K. Fan, R. Riedel, H. Li, J. Sun, H. Li, *Corrosion Science* **231**, 111944 (2024).
10. L. Zhong, L. Guo, J. Huang, N. Liu, Y. Li, H. Li, *Ceramics International* **49(9)**, Part A 13903-13915 (2023).
11. X. Su, Z. Tian, X. Chen, Y. Chen, M. Li, J. Du, Q. Tan, *J. Materials Research and Technology* **18**, 5312-5324 (2022).
12. A.A. Saad, C. Martinez, R.W. Trice, *J. European Ceramic Society* **43(14)**, 6449-6460 (2023).
13. V.V. Alisin, M.N. Roshchin, *Journal of Machinery Manufacture and Reliability* **48(4)**, 361-367 (2019).